J/ψ production cross section and its dependence on charged-particle multiplicity in $p+p$ collisions at $\sqrt{s} = 200$ GeV

STAR Collaboration

J. Adam [i], L. Adamczyk [a], J.R. Adams [ae], J.K. Adkins [u], G. Agakishiev [s], M.M. Aggarwal [ag],
Z. Ahammed [bd], N.N. Ajitanand [ar], I. Alekseev [q,ab], D.M. Anderson [at], R. Aoyama [ax],
A. Aparin [s], D. Arkhipkin [c], E.C. Aschenauer [c], M.U. Ashraf [aw], F. Atetalla [t], A. Attri [ag],
G.S. Averichev [s], X. Bai [g], V. Bairathi [ac], K. Barish [az], A.J. Bassill [az], A. Behera [ar], R. Bellwied [av],
A. Bhasin [r], A.K. Bhati [ag], J. Bielcik [j], J. Bielcikova [k], L.C. Bland [c], I.G. Bordyuzhin [q],
J.D. Brandenburg [al], A.V. Brandin [ab], D. Brown [y], J. Bryslawskyj [az], I. Bunzarov [s],
J. Butterworth [al], H. Caines [bg], M. Calderón de la Barca Sánchez [e], J.M. Campbell [ae],
D. Cebra [e], I. Chakaberia [t,ap], P. Chaloupka [j], F.-H. Chang [ad], Z. Chang [c],
N. Chankova-Bunzarova [s], A. Chatterjee [bd], S. Chattopadhyay [bd], J.H. Chen [aq], X. Chen [ao],
X. Chen [w], J. Cheng [aw], M. Cherney [i], W. Christie [c], G. Contin [x], H.J. Crawford [d], S. Das [g],
T.G. Dedovich [s], I.M. Deppner [ba], A.A. Derevschikov [ai], L. Didenko [c], C. Dilks [ah], X. Dong [x],
J.L. Drachenberg [v], J.C. Dunlop [c], L.G. Efimov [s], N. Elsey [bf], J. Engelage [d], G. Eppley [al],
R. Esha [f], S. Esumi [ax], O. Evdokimov [h], J. Ewigleben [y], O. Eyser [c], R. Fatemi [u], S. Fazio [c],
P. Federic [k], P. Federicova [j], J. Fedorisin [s], P. Filip [s], E. Finch [ay], Y. Fisyak [c], C.E. Flores [e],
L. Fulek [a], C.A. Gagliardi [at], T. Galatyuk [l], F. Geurts [al], A. Gibson [bc], D. Grosnick [bc],
D.S. Gunarathne [as], Y. Guo [t], A. Gupta [r], W. Guryn [c], A.I. Hamad [t], A. Hamed [at],
A. Harlenderova [j], J.W. Harris [bg], L. He [aj], S. Heppelmann [ah], S. Heppelmann [e],
N. Herrmann [ba], A. Hirsch [aj], L. Holub [j], S. Horvat [bg], X. Huang [aw], B. Huang [h], S.L. Huang [ar],
H.Z. Huang [f], T. Huang [ad], T.J. Humanic [ae], P. Huo [ar], G. Igo [f], W.W. Jacobs [p], A. Jentsch [au],
J. Jia [c,ar], K. Jiang [ao], S. Jowzaee [bf], E.G. Judd [d], S. Kabana [t], D. Kalinkin [p], K. Kang [aw],
D. Kapukchyan [az], K. Kauder [bf], H.W. Ke [c], D. Keane [t], A. Kechechyan [s], D.P. Kikoła [be],
C. Kim [az], T.A. Kinghorn [e], I. Kisel [m], A. Kisiel [be], L. Kochenda [ab], L.K. Kosarzewski [be],
A.F. Kraishan [as], L. Kramarik [j], L. Krauth [az], P. Kravtsov [ab], K. Krueger [b], N. Kulathunga [av],
S. Kumar [ag], L. Kumar [ag], J. Kvapil [j], J.H. Kwasizur [p], R. Lacey [ar], J.M. Landgraf [c], J. Lauret [c],
A. Lebedev [c], R. Lednicky [s], J.H. Lee [c], X. Li [ao], C. Li [ao], W. Li [aq], Y. Li [aw], Y. Liang [t], J. Lidrych [j],
T. Lin [at], A. Lipiec [be], M.A. Lisa [ae], F. Liu [g], P. Liu [ar], H. Liu [p], Y. Liu [at], T. Ljubicic [c], W.J. Llope [bf],
M. Lomnitz [x], R.S. Longacre [c], X. Luo [g], S. Luo [h], G.L. Ma [aq], Y.G. Ma [aq], L. Ma [n], R. Ma [c],
N. Magdy [ar], R. Majka [bg], D. Mallick [ac], S. Margetis [t], C. Markert [au], H.S. Matis [x],
O. Matonoha [j], D. Mayes [az], J.A. Mazer [am], K. Meehan [e], J.C. Mei [ap], N.G. Minaev [ai],
S. Mioduszewski [at], D. Mishra [ac], B. Mohanty [ac], M.M. Mondal [o], I. Mooney [bf],
D.A. Morozov [ai], Md. Nasim [f], J.D. Negrete [az], J.M. Nelson [d], D.B. Nemes [bg], M. Nie [aq],
G. Nigmatkulov [ab], T. Niida [bf], L.V. Nogach [ai], T. Nonaka [ax], S.B. Nurushev [ai], G. Odyniec [x],
A. Ogawa [c], K. Oh [ak], S. Oh [bg], V.A. Okorokov [ab], D. Olvitt Jr. [as], B.S. Page [c], R. Pak [c],
Y. Panebratsev [s], B. Pawlik [af], H. Pei [g], C. Perkins [d], J. Pluta [be], J. Porter [x], M. Posik [as],

E-mail address: yezhenyu@uic.edu (Z. Ye).

N.K. Pruthi [ag], M. Przybycien [a], J. Putschke [bf], A. Quintero [as], S.K. Radhakrishnan [x],
S. Ramachandran [u], R.L. Ray [au], R. Reed [y], H.G. Ritter [x], J.B. Roberts [al], O.V. Rogachevskiy [s],
J.L. Romero [e], L. Ruan [c], J. Rusnak [k], O. Rusnakova [j], N.R. Sahoo [at], P.K. Sahu [o], S. Salur [am],
J. Sandweiss [bg], J. Schambach [au], A.M. Schmah [x], W.B. Schmidke [c], N. Schmitz [z],
B.R. Schweid [ar], F. Seck [l], J. Seger [i], M. Sergeeva [f], R. Seto [az], P. Seyboth [z], N. Shah [aq],
E. Shahaliev [s], P.V. Shanmuganathan [y], M. Shao [ao], W.Q. Shen [aq], F. Shen [ap], S.S. Shi [g],
Q.Y. Shou [aq], E.P. Sichtermann [x], S. Siejka [be], R. Sikora [a], M. Simko [k], S. Singha [t],
N. Smirnov [bg], D. Smirnov [c], W. Solyst [p], P. Sorensen [c], H.M. Spinka [b], B. Srivastava [aj],
T.D.S. Stanislaus [bc], D.J. Stewart [bg], M. Strikhanov [ab], B. Stringfellow [aj], A.A.P. Suaide [an],
T. Sugiura [ax], M. Sumbera [k], B. Summa [ah], Y. Sun [ao], X. Sun [g], X.M. Sun [g], B. Surrow [as],
D.N. Svirida [q], P. Szymanski [be], Z. Tang [ao], A.H. Tang [c], A. Taranenko [ab], T. Tarnowsky [aa],
J.H. Thomas [x], A.R. Timmins [av], D. Tlusty [al], T. Todoroki [c], M. Tokarev [s], C.A. Tomkiel [y],
S. Trentalange [f], R.E. Tribble [at], P. Tribedy [c], S.K. Tripathy [o], O.D. Tsai [f], B. Tu [g], T. Ullrich [c],
D.G. Underwood [b], I. Upsal [ae], G. Van Buren [c], J. Vanek [k], A.N. Vasiliev [ai], I. Vassiliev [m],
F. Videbæk [c], S. Vokal [s], S.A. Voloshin [bf], A. Vossen [p], G. Wang [f], Y. Wang [g], F. Wang [aj],
Y. Wang [aw], J.C. Webb [c], L. Wen [f], G.D. Westfall [aa], H. Wieman [x], S.W. Wissink [p], R. Witt [bb],
Y. Wu [t], Z.G. Xiao [aw], G. Xie [h], W. Xie [aj], Q.H. Xu [ap], Z. Xu [c], J. Xu [g], Y.F. Xu [aq], N. Xu [x],
S. Yang [c], C. Yang [ap], Q. Yang [ap], Y. Yang [ad], Z. Ye [h], Z. Ye [h], L. Yi [ap], K. Yip [c], I.-K. Yoo [ak],
N. Yu [g], H. Zbroszczyk [be], W. Zha [ao], Z. Zhang [aq], L. Zhang [g], Y. Zhang [ao], X.P. Zhang [aw],
J. Zhang [w], S. Zhang [aq], S. Zhang [ao], J. Zhang [x], J. Zhao [aj], C. Zhong [aq], C. Zhou [aq], L. Zhou [ao],
Z. Zhu [ap], X. Zhu [aw], M. Zyzak [m]

[a] *AGH University of Science and Technology, FPACS, Cracow 30-059, Poland*
[b] *Argonne National Laboratory, Argonne, IL 60439*
[c] *Brookhaven National Laboratory, Upton, NY 11973*
[d] *University of California, Berkeley, CA 94720*
[e] *University of California, Davis, CA 95616*
[f] *University of California, Los Angeles, CA 90095*
[g] *Central China Normal University, Wuhan, Hubei 430079*
[h] *University of Illinois at Chicago, Chicago, IL 60607*
[i] *Creighton University, Omaha, NE 68178*
[j] *Czech Technical University in Prague, FNSPE, Prague, 115 19, Czech Republic*
[k] *Nuclear Physics Institute AS CR, Prague 250 68, Czech Republic*
[l] *Technische Universitat Darmstadt, Germany*
[m] *Frankfurt Institute for Advanced Studies FIAS, Frankfurt 60438, Germany*
[n] *Fudan University, Shanghai, 200433*
[o] *Institute of Physics, Bhubaneswar 751005, India*
[p] *Indiana University, Bloomington, IN 47408*
[q] *Alikhanov Institute for Theoretical and Experimental Physics, Moscow 117218, Russia*
[r] *University of Jammu, Jammu 180001, India*
[s] *Joint Institute for Nuclear Research, Dubna, 141 980, Russia*
[t] *Kent State University, Kent, OH 44242*
[u] *University of Kentucky, Lexington, KY 40506-0055*
[v] *Lamar University, Physics Department, Beaumont, TX 77710*
[w] *Institute of Modern Physics, Chinese Academy of Sciences, Lanzhou, Gansu 730000*
[x] *Lawrence Berkeley National Laboratory, Berkeley, CA 94720*
[y] *Lehigh University, Bethlehem, PA 18015*
[z] *Max-Planck-Institut fur Physik, Munich 80805, Germany*
[aa] *Michigan State University, East Lansing, MI 48824*
[ab] *National Research Nuclear University MEPhI, Moscow 115409, Russia*
[ac] *National Institute of Science Education and Research, HBNI, Jatni 752050, India*
[ad] *National Cheng Kung University, Tainan 70101*
[ae] *Ohio State University, Columbus, OH 43210*
[af] *Institute of Nuclear Physics PAN, Cracow 31-342, Poland*
[ag] *Panjab University, Chandigarh 160014, India*
[ah] *Pennsylvania State University, University Park, PA 16802*
[ai] *Institute of High Energy Physics, Protvino 142281, Russia*
[aj] *Purdue University, West Lafayette, IN 47907*
[ak] *Pusan National University, Pusan 46241, Republic of Korea*
[al] *Rice University, Houston, TX 77251*
[am] *Rutgers University, Piscataway, NJ 08854*
[an] *Universidade de Sao Paulo, Sao Paulo, 05314-970, Brazil*
[ao] *University of Science and Technology of China, Hefei, Anhui 230026*
[ap] *Shandong University, Jinan, Shandong 250100*
[aq] *Shanghai Institute of Applied Physics, Chinese Academy of Sciences, Shanghai 201800*
[ar] *State University of New York, Stony Brook, NY 11794*
[as] *Temple University, Philadelphia, PA 19122*
[at] *Texas A&M University, College Station, TX 77843*

au *University of Texas, Austin, TX 78712*
av *University of Houston, Houston, TX 77204*
aw *Tsinghua University, Beijing 100084*
ax *University of Tsukuba, Tsukuba, Ibaraki 305-8571, Japan*
ay *Southern Connecticut State University, New Haven, CT 06515*
az *University of California, Riverside, CA 92521*
ba *University of Heidelberg, Heidelberg, 69120, Germany*
bb *United States Naval Academy, Annapolis, MD 21402*
bc *Valparaiso University, Valparaiso, IN 46383*
bd *Variable Energy Cyclotron Centre, Kolkata 700064, India*
be *Warsaw University of Technology, Warsaw 00-661, Poland*
bf *Wayne State University, Detroit, MI 48201*
bg *Yale University, New Haven, CT 06520*

ARTICLE INFO

ABSTRACT

We present a measurement of inclusive J/ψ production at mid-rapidity ($|y| < 1$) in $p+p$ collisions at a center-of-mass energy of $\sqrt{s} = 200$ GeV with the STAR experiment at the Relativistic Heavy Ion Collider (RHIC). The differential production cross section for J/ψ as a function of transverse momentum (p_T) for $0 < p_T < 14$ GeV/c and the total cross section are reported and compared to calculations from the color evaporation model and the non-relativistic Quantum Chromodynamics model. The dependence of J/ψ relative yields in three p_T intervals on charged-particle multiplicity at mid-rapidity is measured for the first time in $p+p$ collisions at $\sqrt{s} = 200$ GeV and compared with that measured at $\sqrt{s} = 7$ TeV, PYTHIA8 and EPOS3 Monte Carlo generators, and the Percolation model prediction.

1. Introduction

Quarkonia are bound states of heavy quark–antiquark pairs ($Q\bar{Q}$). Their production in $p+p$ collisions can be factorized into hard and soft processes associated with short and long distance strong interactions, respectively [1]. The former is related to production of $Q\bar{Q}$ from hard parton scatterings and can be calculated by perturbative Quantum Chromodynamics (pQCD). The latter involves evolution of $Q\bar{Q}$ into bound quarkonium states and is usually parameterized by phenomenological models such as the Color-Evaporation Model (CEM), Color Singlet Model, and Non-Relativistic Quantum Chromodynamics (NRQCD) including both color singlet and octet intermediate states (for a recent review see [2]). With sizable theoretical uncertainties, these model calculations can describe the measurement results of quarkonium production cross sections from the Tevatron and Large Hadron Collider (LHC) experiments [3–6]. Precise measurements of quarkonium production over a wide kinematic range at RHIC energies can provide new constraints on model calculations and insights into the quarkonium production mechanism.

Recent studies at the LHC have revealed a faster-than-linear increase in J/ψ and D-meson relative yields with charged-particle multiplicity (n_{ch}) at mid-rapidity in $p+p$ collisions at $\sqrt{s} = 7$ TeV [7,8], suggesting a strong correlation between hard parton scatterings producing heavy flavor particles and soft underlying processes producing all other particles. By including Multiple-Partonic Interactions (MPI) [9–11], i.e. several interactions at the parton level occurring in a single $p+p$ collision, PYTHIA8 [12] and EPOS3 [13] Monte Carlo (MC) generators can produce an increase in relative yields of heavy flavor particles with n_{ch}, but underestimate the observed yields at large n_{ch} [8]. Additional effects have been suggested to explain the measurement results at the LHC. For example, collective expansion implemented in EPOS3 MC generator [14] is found to modify the p_T distribution of final state particles in high multiplicity $p+p$ collisions at $\sqrt{s} = 7$ TeV, producing a faster-than-linear increase for D-meson relative yields at intermediate

and high p_T [8]. Such an effect is however expected to be small at RHIC energies. On the other hand, the percolation model [15] produces particles through interactions of color strings, which are more suppressed for soft processes than hard processes due to the different size of the color strings. It can also produce a faster-than-linear increase in relative yields of heavy flavor particles with n_{ch} that is qualitatively consistent with the LHC results. Such an increase is predicted to be similar at different energies by the percolation model. Measurements of relative yields of heavy flavor particles versus n_{ch} at RHIC energies can help constrain model calculations and provide knowledge of the energy dependence of MPI in $p+p$ collisions.

In this letter, we present new results of inclusive J/ψ production at mid-rapidity ($|y| < 1$) in $p+p$ collisions at $\sqrt{s} = 200$ GeV with the STAR experiment at RHIC [16]. Both the differential production cross section for J/ψ as a function of transverse momentum (p_T) and the total cross section are obtained with higher precision than the previously published results [17,18]. The dependence of J/ψ relative yields on n_{ch} at mid-rapidity is also determined, for the first time, for $p+p$ collisions at RHIC energies. These results are compared to calculations from various theoretical models and MC generators.

2. STAR experiment and data analysis

The data used in this measurement were collected with minimum-bias (MB) and high-tower (HT) triggers in $p+p$ collisions at $\sqrt{s} = 200$ GeV by the STAR experiment in 2012. The MB triggers select non-single diffractive $p+p$ collisions with a coincidence signal from the two Vertex Position Detectors (VPD) [19] or the two Beam Beam Counters (BBC) [20]. The VPD and BBC are located on both sides of the $p+p$ collision region and covering the pseudo-rapidity region of $4.4 < |\eta| < 4.9$ or $3.3 < |\eta| < 5.0$, respectively. The VPD-triggered MB events are analyzed to study the J/ψ production with $p_T < 1.5$ GeV/c, since the size of the sample (∼300 million, corresponding to an integrated luminosity of about
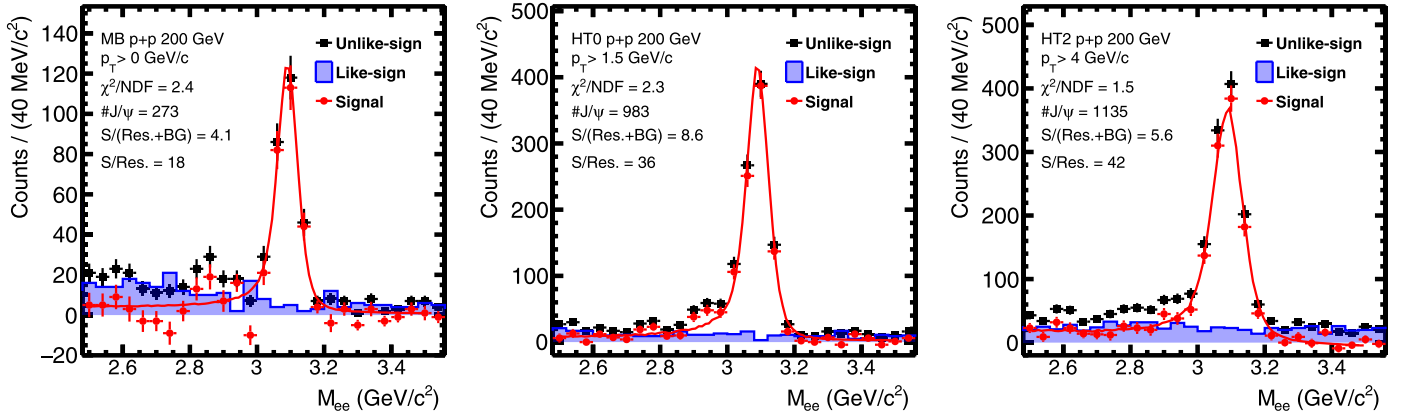
Fig. 1. (Color online.) Invariant mass distributions for unlike-sign pairs (black squares), like-sign pairs (blue histogram), and difference between unlike- and like-sign pairs (red circles) from the VPD- (left), HT0- (middle) and HT2-triggered (right) events in $p+p$ collisions at $\sqrt{s} = 200$ GeV in 2012. The red curve is the combined fit with a Crystal Ball (CB) function and a 1st-order polynomial function representing signal and residual background, respectively.

10 nb^{-1}) is significantly larger than that of the BBC-triggered MB events (about 2.66 million). The latter are used to obtain the n_{ch} distribution in MB $p+p$ collisions, since the BBC has a much higher trigger efficiency than the VPD for low multiplicity $p+p$ collisions. The HT triggers select $p+p$ collisions producing at least one high-p_T particle with large energy deposition in the Barrel Electromagnetic Calorimeter (BEMC) [21]. Data collected by the HT0 (HT2) trigger with an energy threshold of $E_T > 2.6$ (4.2) GeV, corresponding to an integrated luminosity of 1.36 (23.5) pb^{-1}, are analyzed to study J/ψ production with $p_T > 1.5$ (4.0) GeV/c. The vertex positions of $p+p$ collisions along the beam line direction can be reconstructed from TPC tracks (V_z^{TPC}) or from VPD signals (V_z^{VPD}). A cut of $|V_z^{TPC}| < 50$ cm is applied to ensure good TPC acceptance for all the events. An additional cut of $|V_z^{TPC} - V_z^{VPD}| < 6$ cm is applied to reduce the pile-up background from out-of-time collisions for the VPD-triggered MB events.

The main detectors used in the data analysis are the Time Projection Chamber (TPC) [22], Time-Of-Flight detector (TOF) [23], and BEMC, all with full azimuthal coverage within $|\eta| < 1$. The TPC records trajectories of charged particles with $p_T > 0.2$ GeV/c in a 0.5 T solenoid magnetic field and determines their momenta and ionization energy losses (dE/dx). Tracks are required to have a maximum distance of the closest approach to the collision point of 1 cm, a minimum of 20 TPC hits (out of a maximum of 45), and a minimum of 11 TPC hits for dE/dx calculation. The TOF (VPD) provides the stop (start) time of flight information for charged particles from the collision vertices to the TOF, while the BEMC measures electromagnetic energy deposition.

J/ψ candidates are reconstructed through the $J/\psi \rightarrow e^+e^-$ channel, where electrons are identified using the specific energy loss in TPC, dE/dx, the velocity (β) calculated from the path length and time of flight between the collision vertex and TOF, and the ratio between the momentum and energy deposition in the BEMC (pc/E) [17]. The normalized dE/dx is defined as

$$n\sigma_e = \frac{ln(dE/dx) - ln(dE/dx|_{Bichsel})}{\sigma_{ln(dE/dx)}}, \tag{1}$$

where dE/dx ($dE/dx|_{Bichsel}$) is the measured (expected) value, and $\sigma_{ln(dE/dx)}$ is one standard deviation of the $ln(dE/dx)$ distribution. The $n\sigma_e$ value is required to be within $(-1.9, 3)$ for all electron candidates. $|1/\beta - 1| < 0.03$ is required for TOF associated electron tracks, and $0.3 < pc/E < 1.5$ for BEMC-associated candidates with $p_T > 1$ GeV/c. Both daughters of J/ψ candidates are required to pass the $n\sigma_e$ requirement, and either the β or pc/E requirement. For HT-triggered events, at least one daughter of J/ψ candidates must pass the pc/E requirement and have an energy deposition in

the BEMC that is higher than the corresponding HT trigger threshold.

3. J/ψ production cross section

The invariant mass spectra of the reconstructed J/ψ candidates from different triggered samples are shown in Fig. 1. The J/ψ raw yields are extracted by subtracting the invariant mass spectra of like-sign electron pairs ($M_{e^\pm e^\pm}$) from the unlike-sign ones ($M_{e^\pm e^\mp}$). The remaining distribution is fit by a two-component function, composed of a J/ψ signal distribution, the shape of which is obtained from STAR detector simulation [24] with the Crystal-Ball function [25], together with a residual background distribution parameterized by a 1st-order polynomial function. The J/ψ signal to the residual background ratios in the mass range of $2.9 < M_{ee} <$ 3.2 GeV/c^2 are 18, 36, and 42 for the VPD MB, HT0 and HT2 data, respectively, and have negligible dependence on n_{ch}. The large values of this ratio reflect that the residual background is small and can be neglected for the measurement of the n_{ch}-dependence of J/ψ relative yields.

The J/ψ production cross sections are obtained by correcting the J/ψ raw yields for the detector geometric acceptance and efficiency. The vertex finding, track reconstruction, BEMC electron identification, VPD, BBC and HT trigger efficiencies are estimated from detector simulation, while the electron identification efficiencies by TPC dE/dx and TOF $1/\beta$ requirements are estimated from data. The cross sections from the VPD MB, HT0 and HT2 data are consistent with each other in the overlapping p_T regions, and are used for $0 < p_T < 1.5$, $1.5 < p_T < 4.0$ and $4.0 < p_T < 14$ GeV/c, respectively. Here unpolarized J/ψ is used in simulation when calculating the J/ψ acceptance and efficiency, which is around 20% for the VPD MB data, 0.6–12% for the HT0 data, and 1.5–30% for the HT2 data, respectively. The latter two increase as a function of J/ψ p_T due to the increasing HT trigger efficiency.

The total systematic uncertainty for the measured cross section is obtained from the square root of the quadratic sum of the individual systematic uncertainties listed in Table 1, which generally depend on the J/ψ signal significance in each p_T bin. The uncertainty in the raw J/ψ yield extraction, estimated by varying the fitted mass range, by changing the residual background shape from a 1st-order polynomial function to an exponential function, and by comparing the fit result to the bin counts in $2.9 < M_{ee} <$ 3.2 GeV/c^2 corrected for the residual background and for the invariant mass cut efficiency, is between 1–14%. The uncertainties in the track reconstruction and electron identification efficiencies, estimated by varying the corresponding cuts in data and simulation,

Table 1

Systematic uncertainties for the measurement of the J/ψ production cross section. See text for details.

Type	Uncertainty (%)
Raw yield extraction	1–14
Tracking efficiency	3–15
Electron identification efficiency	4–14
TOF-EMC efficiency correlation	1–7
HT trigger efficiency	4–13 (HT)
Normalization	10 (MB)
	8.5 (HT)

are 3–15% and 4–14%, respectively. Since the TOF efficiency is calculated from tracks matched with BEMC hits, there is a correction applied to the TOF efficiency by the ratio of true TOF efficiency to that calculated with BEMC-matched tracks. This correction causes an uncertainty of 1–7%. The HT trigger efficiency uncertainty, estimated by varying the trigger requirement in data and simulation, is 4–13%. An 8% normalization uncertainty due to the luminosity determination is applied for both the MB and HT results. An additional 6% (3%) normalization uncertainty for the VPD MB (HT) result is added for the VPD (BBC) trigger and vertex reconstruction efficiency, making the total normalization uncertainty 10% (8.5%).

Fig. 2 shows the measured J/ψ production cross section times the $J/\psi \to e^+e^-$ branching ratio (B_{ee}) as a function of J/ψ p_T. The new result is consistent with the published STAR [17] result, but has better statistical precision for $p_T < 10$ GeV/c. It is also consistent with the published PHENIX [18] result, but has better precision for $p_T > 2$ GeV/c. The total J/ψ production cross section times the branching ratio per rapidity unit is estimated to be

$$B_{ee}\frac{d\sigma}{dy}|_{y=0} = 43.2 \pm 3.0(stat.) \pm 7.5(syst.) \text{ nb}. \tag{2}$$

Also shown in Fig. 2 are theoretical model calculations. The green band represents the result from CEM calculations for $0 < p_T < 14$ GeV/c and $|y| < 0.35$ [3], the orange band shows that from Next-to-Leading Order (NLO) NRQCD calculations for $4 < p_T < 14$ GeV/c and $|y| < 1$ [4], the blue band depicts the result from NRQCD calculations for $0 < p_T < 5$ GeV/c and $|y| < 1$ which incorporates a Color-Glass Condensate (CGC) effective theory framework for small-x resummation [26], and the magenta band shows that from NLO NRQCD calculations for $1.1 < p_T < 10$ GeV/c and $|y| < 0.35$ [5]. The CEM and NLO NRQCD calculations describe the data reasonably well for the applicable p_T ranges. The CGC+NRQCD calculations are consistent with the data within uncertainties, however, the data are close to the lower uncertainty boundary of the theoretical calculation. We note that the feed-down contributions from higher charmonium states χ_{cJ} and $\psi(2S)$ are explicitly considered by the calculations in Refs. [4,26], but not by the calculations in Refs. [3,5] where model parameters have been fit to inclusive J/ψ cross sections from experimental measurements. We also note that the feed-down contribution from bottom hadron decays is included in the experimental data but not included in any of these calculations, which is predicted to be approximately 10–25% in the range of $4 < p_T < 14$ GeV/c [27,28]. As can be seen, except for the two bins at the highest p_T, the uncertainties in the experimental results are smaller than those in the theoretical calculations. Therefore, the new STAR result can be used to constrain theoretical model calculations.

4. Dependence of J/ψ production on n_{ch}

The BBC-triggered MB data are used to characterize the n_{ch} distribution at mid-pseudorapidity ($|\eta| < 1$) in MB $p+p$ collisions. The n_{ch} distribution for $p+p$ collisions producing J/ψ is obtained
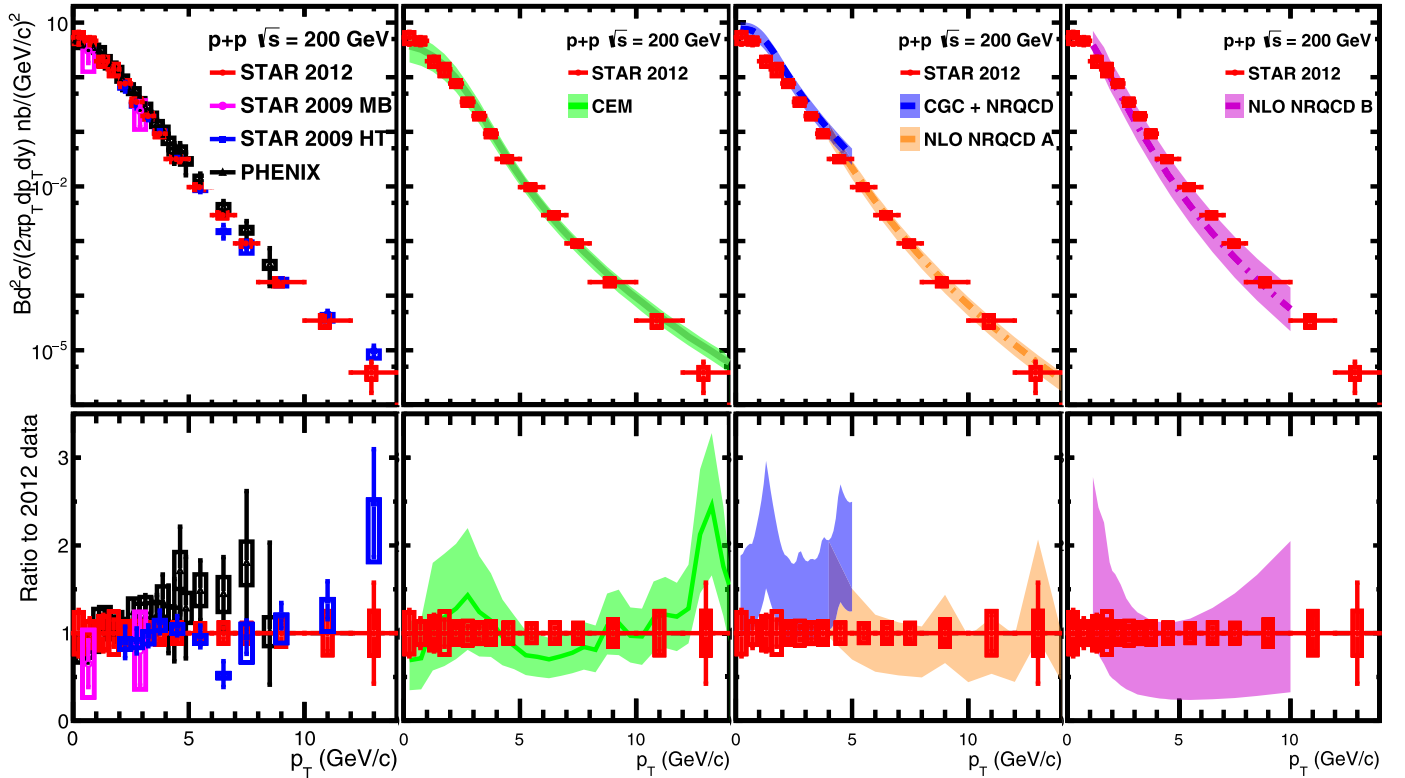
Fig. 2. (Color online.) Top: J/ψ cross section times branching ratio as a function of p_T in $p+p$ collisions at $\sqrt{s} = 200$ GeV. Solid circles are from this analysis for $|y| < 1$; open circles and blue squares are the published results for $|y| < 1$ from STAR [17]; triangles are the published results for $|y| < 0.35$ from PHENIX [18]. Bars and boxes are statistical and systematic uncertainties, respectively. The curves are CEM (green) [3], NLO NRQCD A (orange) [4], CGC+NRQCD (blue) [26], and NLO NRQCD B (magenta) [5] theoretical calculations, respectively. Bottom: ratios of these results with respect to the central value from this analysis.
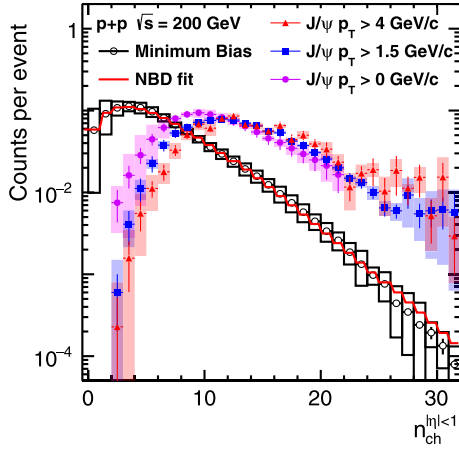
Fig. 3. (Color online.) The corrected n_{ch} distributions at mid-rapidity ($|\eta| < 1$) for MB events (open circles) and J/ψ events with J/ψ p_T greater than 0 (purple circles), 1.5 (blue squares), and 4 GeV/c (red triangles) in $p+p$ collisions at $\sqrt{s} = 200$ GeV. The fit function is a negative binomial function. Bars and boxes are statistical and systematic uncertainties, respectively.

by subtracting the n_{ch} distribution of events containing like-sign electron pairs with $2.9 < M_{ee} < 3.2$ GeV/c^2 from that of unlike-sign pairs, both of which are reweighted by the inverse of the J/ψ reconstruction efficiency. Here the raw n_{ch} for each event is obtained from the number of tracks reconstructed in the TPC with a matched hit in the TOF. Unlike the TPC, which is suscepti-ble to pile-up tracks from out-of-time collisions, the TOF only records signals from particles produced from the triggered colli-sion. About 1% of tracks from out-of-time collisions may randomly match a TOF hit and the effect of these pile-up tracks is considered as a systematic uncertainty. The raw n_{ch} distributions are corrected for the trigger and vertex finding efficiencies, which are important for low multiplicity $p+p$ collisions, and for the TPC and TOF ac-ceptances and efficiencies through an iterative Bayesian unfolding method [29]. The response matrix used for unfolding is obtained from MC samples generated with PYTHIA8.183 [12] and convoluted with the detector acceptances and efficiencies. Here the true n_{ch} in the response matrix is defined as the number of charged parti-cles produced promptly from the primary vertex, including pion, kaon, proton, electron, and muon with $|\eta| < 1$, $p_T > 0$ GeV/c, and not from K^0 or Λ decays. In addition, J/ψ events require that the J/ψ-decay electrons are within $|\eta| < 1$ and included in the n_{ch} calculations.

Fig. 3 shows the corrected n_{ch} distributions, together with a negative binomial distribution (NBD) function fitted to the distri-bution in MB $p+p$ collisions. The average charged-particle mul-tiplicity per pseudo-rapidity unit obtained from the fit, $\langle dN_{ch}^{MB}/d\eta\rangle = 2.9 \pm 0.3(stat.) \pm 0.2(model) \pm 0.4(syst.)$, is consistent with the previous STAR published result [24]. The model uncertainty is estimated from the difference between the average value of the n_{ch} distribution and the NBD fit result. As can be seen, the average n_{ch} for $p+p$ collisions producing J/ψ increases with increasing J/ψ p_T and is higher than that for MB collisions.

The corrected n_{ch} distributions are divided into five inter-vals: 0–5, 6–10, 11–15, 16–21 and 22–31. The J/ψ relative yield $N_{J/\psi}/\langle N_{J/\psi}\rangle$ and relative charged-particle multiplicity $(dN_{ch}^{MB}/d\eta)/\langle dN_{ch}^{MB}/d\eta\rangle$ are estimated for each interval, where $N_{J/\psi}$ is the number of J/ψ produced per MB collision in a multi-plicity interval, and $\langle N_{J/\psi}\rangle$ the average value over the whole multiplicity range. The last bin in MB events is excluded due to the large statistical uncertainty. The systematic uncertainties for $(dN_{ch}^{MB}/d\eta)/\langle dN_{ch}^{MB}/d\eta\rangle$ and $N_{J/\psi}/\langle N_{J/\psi}\rangle$ are summarized in

Table 2
Systematic uncertainties for the measurement of the dependence of J/ψ relative yields on n_{ch}. See text for details.

Type	Uncertainty (%)	
	$\dfrac{dN_{ch}^{MB}/d\eta}{\langle dN_{ch}^{MB}/d\eta\rangle}$	$\dfrac{N_{J/\psi}}{\langle N_{J/\psi}\rangle}$
Vertex finding	2	3
Tracking	4–5	4–23
Unfolding	2–7	1–30
Pile-up	2	1–10

Table 2. The vertex finding efficiency correction has 3% uncer-tainty, estimated by the difference between the default PYTHIA8 tune and the STAR heavy flavor tune [30]. The track reconstruction efficiency correction is obtained from detector simulation. It de-pends on n_{ch} and has 4–5% uncertainty for MB events and 4–23% uncertainty for J/ψ events. The unfolding process uncertainty is studied by changing the number of Bayesian unfolding iterations and the PYTHIA tune, and by reweighting PYTHIA n_{ch} distribution to match with the unfolded n_{ch} distribution from data. This un-certainty is found to be 2–7% and 1–30% for MB and J/ψ events, respectively. The effect of pile-up track contributions is estimated by the difference between the NBD fit and the actual n_{ch} dis-tribution in MB $p+p$ collisions, as well as by the difference in the n_{ch} distribution between the lowest and highest Zero-Degree Calorimeter (ZDC) [31] coincidence rate. The ZDC rate ranged be-tween 1–13 kHz and is proportional to the instantaneous luminos-ity. The uncertainty due to pile-up track contributions is 2% and 1–10% for MB and J/ψ events, respectively.

Fig. 4 shows the dependence of the J/ψ relative yield on the relative charged-particle multiplicity for J/ψ $p_T > 0$, 1.5 and 4 GeV/c, respectively. A strong increase in J/ψ relative yields with n_{ch} is observed, which seems to be stronger at higher p_T as suggested by data. The result for J/ψ relative yield with $p_T > 0$ GeV/c in $p+p$ collisions at $\sqrt{s} = 200$ GeV is compared with that at $\sqrt{s} = 7$ TeV [7]. The two results follow a similar trend despite more than one order of magnitude difference in $\sqrt{s}$, sug-gesting a weak dependence of the underlying mechanism on $\sqrt{s}$. Also shown in Fig. 4 are calculations from different MC generators and the percolation model. PYTHIA8.183 [12] with the color recon-nection scenario describes MPI through pQCD, taking into account the dependence on the energy and impact parameter (the distance between the colliding protons in the plane perpendicular to the beam direction) of $p+p$ collisions. It can describe the J/ψ rela-tive yield and predicts stronger increase of the J/ψ relative yield with n_{ch} at higher p_T. EPOS3 [13] uses a Gribov–Regge multi-ple scattering framework to describe initial $p+p$ collisions and thus includes MPI in both hard and soft processes. Furthermore, it incorporates features of hydrodynamical evolution [14] in high-multiplicity $p+p$ collisions, which is suggested to be important for $p+p$ collisions at $\sqrt{s} = 7$ TeV [8] but has little effect at $\sqrt{s} = 200$ GeV. Because EPOS3 does not implement J/ψ production, we compare our data with the prediction from EPOS3 on the open charm production. The latter for $2 < p_T < 4$ ($4 < p_T < 8$) GeV/c is found to be in good agreement with the STAR J/ψ result for $p_T > 1.5$ ($p_T > 4$) GeV/c. The Percolation model [15] adapts a framework of color string interactions to describe $p+p$ collisions. In a high-density environment, the coherence among the sources of the color strings leads to a reduction of their effective number. The total charged-particle multiplicity, which originates from soft sources, is more reduced than heavy-particle production for which the sources have a smaller transverse size. The Percolation model prediction is consistent with the data for $p_T > 0$ GeV/c.
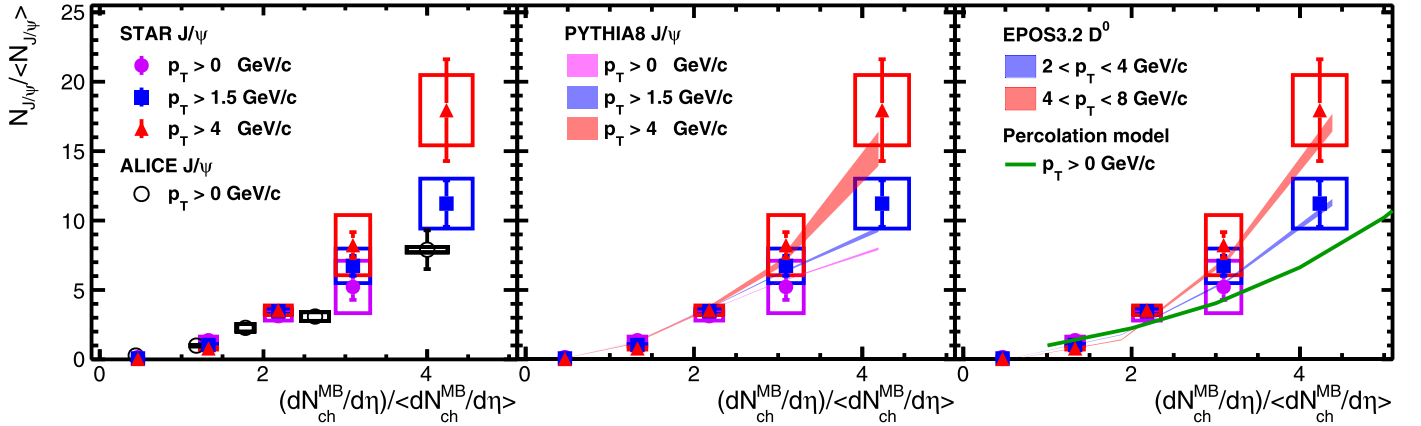
Fig. 4. (Color online.) The multiplicity dependence of J/ψ production in $p+p$ collisions at $\sqrt{s} = 200$ GeV. Purple circles, blue squares, and red triangles represent the results for J/ψ with p_T greater than 0, 1.5, and 4 GeV/c, respectively. Bars and open boxes are statistical and systematic uncertainties, respectively. The ALICE result [7] is shown in the left panel. The purple, blue and red bands in the middle panel are generated from PYTHIA8 for J/ψ with p_T greater than 0, 1.5, and 4 GeV/c, respectively. The blue and red bands in the right panel are from EPOS3 model calculations for D^0 with $2 < p_T < 4$ and $4 < p_T < 8$ GeV/c, respectively, while the green curve is from the Percolation model for J/ψ with $p_T > 0$ GeV/c.

5. Summary

In summary, inclusive J/ψ production at mid-rapidity $|y| < 1$ in $p+p$ collisions at $\sqrt{s} = 200$ GeV is studied through the $J/\psi \to e^+e^-$ channel with the STAR experiment. The measured differential production cross section as a function of J/ψ p_T can be described within experimental and theoretical uncertainties by CEM calculations for $0 < p_T < 14$ GeV/c, NLO NRQCD calculations for $4 < p_T < 14$ GeV/c, and CGC+NRQCD calculations for $0 < p_T < 5$ GeV/c. The total J/ψ production cross section per rapidity unit times $J/\psi \to e^+e^-$ branching ratio is $43.2 \pm 3.0(stat.) \pm 7.5(syst.)$ nb. The J/ψ relative yield is found to increase with charged-particle multiplicity at mid-rapidity. The increase is stronger than a linear rise, and seems to depend on J/ψ p_T but weakly on the center-of-mass energy of the $p+p$ collisions when compared to the experimental result at $\sqrt{s} = 7$ TeV. The increase can be described by PYTHIA8 and EPOS3 MC generators taking into account Multiple-Partonic Interactions, and by the Percolation model.

Acknowledgements

References

[1] G.C. Nayak, J.-W. Qiu, G. Sterman, Phys. Lett. B 613 (2005) 45;
G.C. Nayak, J.-W. Qiu, G. Sterman, Phys. Rev. D 72 (2005) 114012;
G.C. Nayak, J.-W. Qiu, G. Sterman, Phys. Rev. D 74 (2006) 074007.
[2] A. Andronic, et al., Eur. Phys. J. C 76 (2016) 107.
[3] A.D. Frawley, T. Ullrich, R. Vogt, Phys. Rep. 462 (2008) 125, and R. Vogt private communication (2009).
[4] Y.-Q. Ma, K. Wang, K.-T. Chao, Phys. Rev. D 84 (2011) 114001.
[5] M. Butenschoen, B.A. Kniehl, Phys. Rev. Lett. 108 (2012) 172002.
[6] B. Gong, L.-P. Wan, J.-X. Wang, H.-F. Zhang, Phys. Rev. Lett. 110 (2013) 042002.
[7] B. Abelev, et al., ALICE collaboration, Phys. Lett. B 712 (2012) 165.
[8] J. Adam, et al., ALICE collaboration, J. High Energy Phys. 09 (2015) 148.
[9] P. Bartalini, L. Fano, in: P. Bartalini, L. Fano (Eds.), 1st International Workshop on Multiple Partonic Interactions at the LHC (MPI@LHC08), Perugia, Italy, 27–31 October 2008, DESY, Hamburg, 2009, arXiv:1003.4220.
[10] T. Sjöstrand, M. van Zijl, Phys. Rev. D 36 (1987) 2019.
[11] S. Porteboeuf, R. Granier de Cassagnac, Nucl. Phys. Proc. Suppl. 214 (2011) 181.
[12] T. Sjöstrand, S. Mrenna, P. Skands, Comput. Phys. Commun. 178 (2008) 852.
[13] H.J. Drescher, M. Hladik, S. Ostapchenko, T. Pierog, K. Werner, Phys. Rep. 350 (2001) 93.
[14] K. Werner, B. Guiot, I. Karpenko, T. Pierog, Phys. Rev. C 89 (2014) 064903.
[15] E.G. Ferreiro, C. Pajares, Phys. Rev. C 86 (2012) 034903.
[16] K. Ackermann, et al., Nucl. Instrum. Methods A 499 (2003) 624.
[17] L. Admaczyk, et al., STAR collaboration, Phys. Lett. B 722 (2013) 55;
L. Admaczyk, et al., STAR collaboration, Phys. Rev. C 93 (2016) 064904.
[18] A. Adare, et al., PHENIX collaboration, Phys. Rev. D 82 (2010) 012001.
[19] W. Llope, et al., Nucl. Instrum. Methods A 522 (2004) 252.
[20] J. Kiryluk, AIP Conf. Proc. 675 (2003) 424.
[21] M. Beddo, et al., Nucl. Instrum. Methods A 499 (2003) 725.
[22] M. Anderson, et al., Nucl. Instrum. Methods A 499 (2003) 659.
[23] B. Bonner, et al., Nucl. Instrum. Methods A 508 (2003) 181.
[24] B.I. Abelev, et al., STAR collaboration, Phys. Rev. C 79 (2009) 034909.
[25] T. Skwarnicki, DESY F31-86-02, 1986.
[26] Y.-Q. Ma, R. Venugopalan, Phys. Rev. Lett. 113 (2014) 192301.
[27] M. Bedjidian, et al., arXiv:hep-ph/0311048, 2004.
[28] M. Cacciari, P. Nason, R. Vogt, Phys. Rev. Lett. 95 (2005) 122001.
[29] G. D'Agostini, Nucl. Instrum. Methods A 362 (1995) 487.
[30] L. Adamczyk, et al., STAR collaboration, Phys. Rev. D 86 (2012) 072013.
[31] C. Adler, et al., Nucl. Instrum. Methods A 470 (2001) 488.